ISSN 1330-3651 (Print), ISSN 1848-6339 (Online) https://doi.org/10.17559/TV-20240201001306
Original scientific paper

Co-Stand: Swashplateless Micro Aerial Robot Test Stand

Ali Tahir KARASAHIN*, Gokhan GUNGOR

Abstract: Micro aerial robots are mainly employed for tasks in indoor environments where high maneuverability is required, particularly in navigating complex and constrained spaces with numerous closely positioned obstacles. Swashplateless mechanisms can reduce noise, increase operational efficiency, and enhance maneuverability, enabling agile and precise movements in indoor operations. This paper introduces a test stand, called Co-Stand, designed to evaluate the performance of the micro aerial robots equipped with the swashplateless mechanisms using ground-based testing, without requiring actual flight tests. The Co-Stand is constructed to collect data on operational performance to investigate the design criteria of the swashplateless mechanisms. The experiments performed on the Co-Stand are used to evaluate both the swashplateless and standard propeller design performances. The results demonstrate that the swashplateless mechanisms achieve the performance criteria of the standard propellers, showcasing their advantages in indoor environments.

Keywords: coaxial helicopter; micro aerial robot; swashplateless mechanism; test stand

1 INTRODUCTION

Unmanned aerial vehicles (UAVs) offer a simple, high-performance, and cost-effective solution for a wide range of applications, including monitoring and maintenance of power lines, transportation of suspended loads, greenhouse monitoring, and aerial manipulation, enhancing both efficiency and versatility [1-5]. They can feature different motor-propeller configurations for specific task needs and conditions [6] and are expected to exhibit similar capabilities in indoor environments. Micro aerial robots (MARs) are designed for indoor environments, known for their adeptness in navigating complex spaces, compact size, and high maneuverability. MARs, such as coaxial helicopters [7, 8], robotic hummingbirds [9], and quadcopters [10], offer unique advantages for hovering and maneuverability in constrained spaces. Coaxial helicopters have advantages over other types of aircraft for performing specified precision missions in indoor environments. Quadcopters are defined as underactuated since they have six degrees of freedom (DoF) and perform position and orientation movements through four motors. Therefore, it has some disadvantages for precise positioning in an indoor environment. To cope with this challenge, either additional motors are required to produce rotational motion to the points where the motors are connected, or the number of motors used from the aircraft is increased [11]. In both cases, the solution increases the complexity and cost of the system. In coaxial helicopters, which are capable of precise positioning in the indoor environment due to their hovering capability, there is a dependence on the tail and swashplate mechanism [12]. To handle the disadvantages of coaxial helicopters, the swashplateless passive mechanism was designed [13]. In this way, the design and manufacturing capabilities of coaxial helicopters are facilitated and the cost of the swashplate in the mass budget is saved to the payload. The developed design not only eliminates the dependency on the swashplate, but also allows the generation of orientation motions in the pitch and roll axes with the thrust of a single motor. The feasibility of using the swashplateless passive mechanism in a coaxial helicopter has been demonstrated in a flight test [14]. The coaxial helicopter used during the test did not use any aerodynamic control surfaces or extra actuators. The proposed design is compared with the conventional quadcopter and swashplate coaxial helicopter according to the mass distribution of the subsystems. The simplicity and mass advantage of the swashplateless design is expressed. There is also an example of the use of two coaxial motors with a swashplateless passive mechanism in an aircraft [15]. In this case, the coaxial helicopter is defined as fully actuated. In this study, the forces and moments are generated in six DoF using only two actuators with swashplateless passive mechanism. With the swashplateless passive mechanism, both pitch and roll angle changes are designed to allow the propellers to move around two hinges in the passive mechanism. The actuators are also driven accordingly for these orientations to occur [15, 16]. The simplicity, reliability, and cost-effectiveness of the swashplateless passive mechanism allow for different types of aircraft designs. With the passive cyclic pitch varying mechanism used in the Gemini II servoless bi-copter, various aggressive maneuvers were successfully performed using only two actuators [17]. Various experiments have been performed for wind gust disturbance, obstacle avoidance and flight efficiency with the HALO swashplateless mechanism designed as coaxial and dual-ducted. According to the results obtained, it has been shown that HALO has the potential to be used in various applications in terms of robustness and safety characteristics [18]. A vertical takeoff and landing (VTOL) UAV was developed using a swashplateless mechanism. Various tests have shown that the swashplateless mechanism without pitch and yaw elevons can be used in a VTOL type aircraft [19]. Autonomous navigation tasks were performed with the swashplateless mechanism used in a self-rotating and single-actuated aerial robot. The swashplateless mechanism provides a 26.7% decrease in power consumption compared to its counterparts while performing tasks with a simple structure and reduced hardware dependency [20]. As a result, the experimentations executed with the swashplateless mechanism reveal its potential to improve the capabilities of existing aircraft designs. Constructing a test stand is important for conducting comprehensive performance evaluations and control tests of aerial robots. The main contribution of this paper is the development of a test stand

for MARs with swashplateless mechanism. Utilizing the Co-Stand testbed enables comprehensive evaluation of swashplateless mechanisms, without actual flight testing. Moreover, the proposed testbed allows proper examination and optimization of aerial robotics, assuring sufficient functionality and reliability in different operating strategies. Performance evaluation of many recent studies mostly relies on actual flight testing, but they are resource intensive and less regulated. Our research presents the Co-Stand testbed, promoting comprehensive evaluation of the swashplateless mechanism via ground-based testing alone. The proposed approach allows for accurate measurement and analysis of performance benchmarks without requiring actual flight testing, thereby delivering a more efficient, regulated, and cost-effective technique for aerial robot technology. In addition, through rigorous ground-based testing, this research validates the effectiveness of swashplateless mechanisms, significantly advancing aerial robot technology and its applications in various indoor environments, particularly for tasks such as infrastructure inspection, precision agriculture, search and rescue operations, construction, and environmental monitoring. The article is organized as follows: In Section 2, the working principle and design criteria of the swashplateless mechanism are discussed. In Section 3, the kinematic model of the swashplateless mechanism is obtained. The kinematic model needs to be obtained for the applications for controlling the actuator used in the swashplateless mechanism. In Section 4, the results obtained from the experiments performed on the test stand are shared. In Section 5, the results obtained from the experiments performed on the designed test stand are evaluated.

2 SWASHPLATELESS MECHANISM AND TEST STAND

In this section we will describe the working principles, design criteria and the test stand designed for the swashplateless mechanism invented by Paulos et al [13].

2.1 Swashplateless Mechanism

The passive mechanism that allows obtaining orientation movements as well as position movements from a single actuator is shown in Fig. 1.

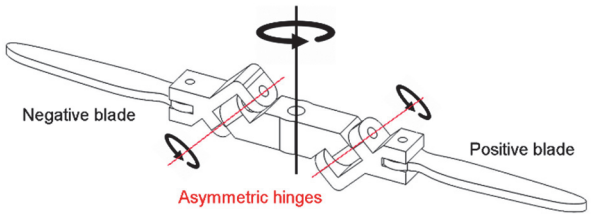

Figure 1 Passive mechanism added between the propellers

The swashplateless mechanism is added between the propellers as a passive element. This mechanism consists of three parts. These are the main body connected to the actuator and the parts holding the positive and negative blades. The main body in the passive mechanism transmits the rotational motion produced in the actuator to the mechanism. The main body and the blades are connected to each other at a certain hinge angle. This hinge angle allows the pitch angle obtained from the mechanism to be produced. Determining the ideal hinge angle is a very important design criterion in swashplateless mechanism design. The degrees of freedom that allow roll and pitch movements to occur with the passive mechanism are shown in Fig. 2.

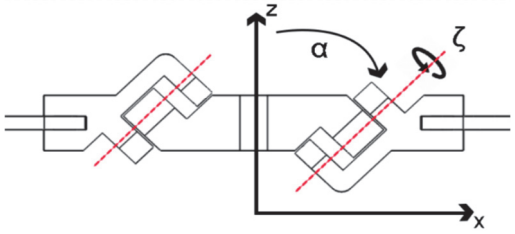

Figure 2 Front view of passive mechanism

The main body of the passive mechanism and the parts holding the propellers are connected to each other at a certain angle (α). The lag angle (ζ) occurs when pitch and roll motion occurs. The lag angle value (ζ) is formed depending on the mechanical limits in the passive mechanism design and the signal used during the actuator drive. The pitch angle that will occur in the passive mechanism when a sinusoidal throttle signal is generated is shown in Fig. 3.

Figure 3 Change of propellers in case of pitch angle

As the positive propeller moves forward, the pitch angle will decrease, whereas if it moves backwards, the pitch angle will increase. The generation of the pitch angle in the passive mechanism is entirely related to the sinusoidal throttle signal applied to the actuator. The test stand designed in this study is shown in Fig. 4.

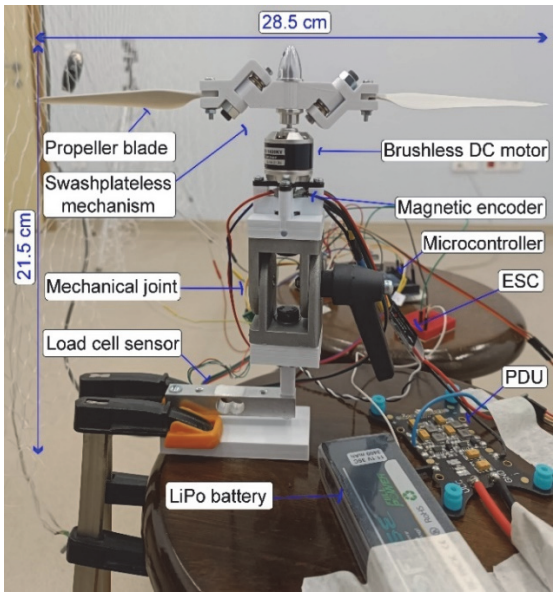

Figure 4 Co-Stand: Swashplateless mechanism test stand

2.2 Test Stand and Hardware

The swashplateless mechanism consisting of the main body and propeller holders was 3D printed using polylactic acid (PLA) material. Emax XA2212 1400KV brushless DC motor (BLDC) was preferred as the actuator used in the passive mechanism. The size of the propeller used in the actuator was 8.46x1. AS5600 magnetic encoder was used to obtain the rotor position angle of the actuator. The magnetic encoder was also used to determine the angular velocity information. A 30A LittleBee BLHeli electronic speed controller (ESC) was used to drive the BLDC motor. There is a mechanical joint in the test stand to allow orientation movement because of the sinusoidal throttle signal. Thus, there is also a capability that allows attitude control applications over the test stand. There is also a load cell sensor to measure the thrust force obtained from the actuator during the test. The energy required for the actuator and microcontroller during the test is obtained from an 11.1 V 3.4 Ah LiPo battery. The supply voltages of the electronic equipment used in the test stand are provided through the power distribution unit (PDU). The power consumption of the actuator connected to the test stand is calculated via the ACS712 current sensor and a voltage divider circuit. The data obtained from the test stand is sent to the computer via serial communication via Atmel ATmega2560 8-bit microcontroller and the received data is recorded in the computer environment.

3 KINEMATIC MODEL OF PASSIVE MECHANISM

Consider a passive mechanism representation, as shown in Fig. 2. There exists a ground-fixed inertial frame. x and z are orthogonal directions with z rotated 90° counter-clockwise from x, and y completes the right hand rule. The lag-pitch hinge coordinate is shown with a red colour dashed line with an angle α. The rotation along the lag-pitch coordinate is represented by ξ called lag angle. The direction of the lag-pitch hinge coordinate with the lag angle can be written in term of ground frame components as:

$$w = \left[\sin(\alpha)x \quad 0 \quad -\cos(\alpha)z\right]^T \tag{1}$$

Any lag rotation ξ about the lag-pitch hinge coordinate w is descried by the rotation matrix with a first-order approximation as:

$$\exp(\hat{w}\xi) = I + \hat{w}d\xi \tag{2}$$

where I is the identity matrix, $\hat{w}$ is the skew symmetric matrix, $d\xi$ is the infinitesimal rotation size.

4 EXPERIMENTAL RESULTS OF THE SWASHPLATE MECHANISM

The tests of the swashplateless passive mechanism were carried out on the developed test stand named Co-Stand. The swashplateless passive mechanism tested with Co-Stand is shown in Fig. 5.

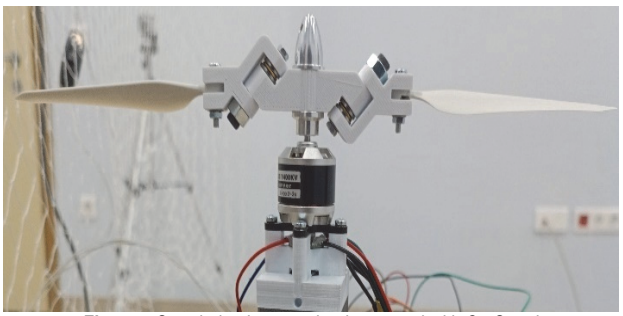

Figure 5 Swashplateless mechanism tested with Co-Stand

A new design was realized by Chen et al. to reduce friction in the swashplateless mechanism and to prevent axis shifts at the hinge point [20] With the Co-Stand developed within the scope of this study, the swashplateless mechanism designed to reduce friction was used. In the swashplateless passive mechanism, in addition to the previous designs, bearings are used at the hinge point in the main body to prevent axial shifts, and pressure bearings are used to carry the shifts and axial forces in the propeller holder parts With the Co-Stand, both the swashplateless passive mechanism and the solid rotor were tested. Thus, it is shown that the swashplateless mechanism can produce the performances obtained from standard propellers. The tests were compared with throttle signals applied to two different propeller mechanisms with constant throttle signals. The data obtained because of the throttle signal applied as 17% is shown in Fig. 6.

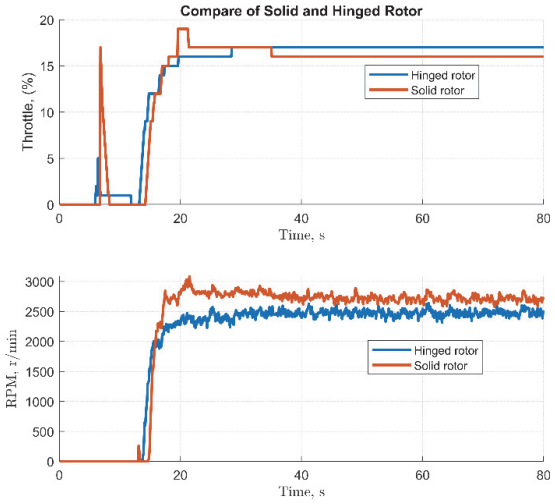

Figure 6 RPM result obtained against constant throttle (17%) signal

According to the results of the experiment carried out on the Co-Stand, it was observed that the swashplateless mechanism reached an average value of 2500 RPM. The standard propeller reached 2700 RPM. The thrust forces generated in case of a constant throttle signal are shown in Fig. 7.

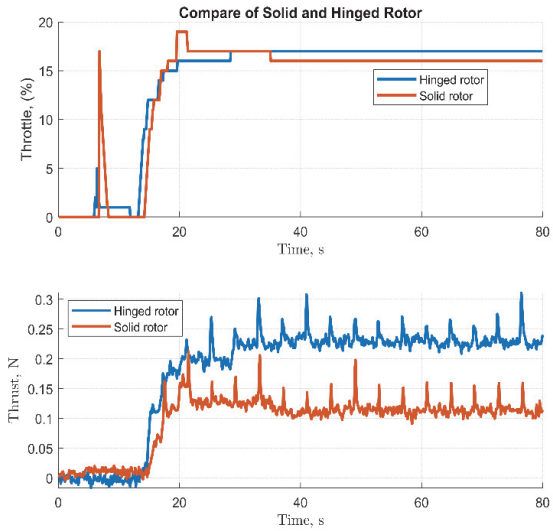

Figure 7 Thrust force result obtained against constant throttle (17%) signal

According to the data obtained from the force sensor on the Co-Stand, the standard propeller produced 0.11 N thrust force against a throttle signal applied at 17%. In the same test, the swashplateless mechanism was shown to produce a thrust force of 0.22 N. The tests on the Co-Stand were repeated with different throttle signals. The results obtained as a result of the throttle signal applied as 23% are shown in Fig. 8.

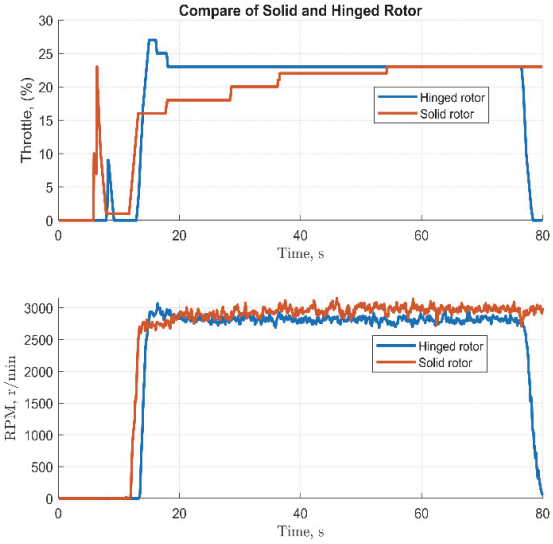

Figure 8 RPM result obtained against constant throttle (23%) signal

In the case of a constant throttle signal, the standard propeller reaches 3000 RPM while the swashplateless passive mechanism reaches 2800 RPM. The results of the thrust force measured with the Co-Stand in the case of 23% throttle signal are shown in Fig. 9.

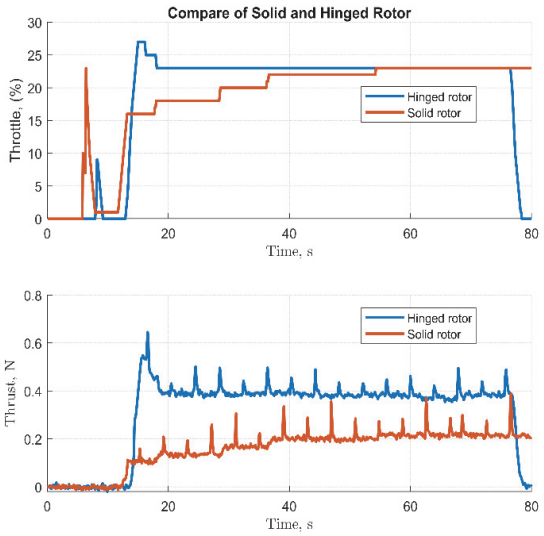

Figure 9 Thrust force result obtained against constant throttle (23%) signal

According to the data obtained, the solid rotor mechanism produced a thrust force value of 0.19 N, while the hinged rotor mechanism produced a thrust force of 0.38 N. The power consumption of the actuator when two different throttle signals are applied is shown in Tab. 1.

Table 1 Electrical power consumption in tests with various throttle signal

Throttle Signal / %	Solid Rotor / W	Hinged Rotor / W
17	3.94	6.38
23	7.57	12.34

Experimental studies were carried out with two different propeller mechanisms and two different constant throttle signals. According to the results obtained, the swashplateless mechanism can reach the RPM and thrust force values of the standard propeller. While reaching these values, no mechanical and electronic problems were encountered.

5 CONCLUSION

The proposed Co-Stand test stand proves its practicality for assessing swashplateless mechanism design criteria without the need for actual flight testing. The experimental results show that swashplateless mechanisms perform comparably to standard propellers, offering reduced power consumption, better maneuverability, and quieter operation. Moreover, the results indicate that adopting the swashplateless mechanisms in aerial robotics could improve operational efficiency, reduce maintenance costs, and enhance reliability, promising industrial applications such as monitoring large indoor facilities, infrastructure inspection, and warehouse management. Future research will investigate various design criteria variations and implement attitude control applications using the Co-Stand test stand, thereby advancing capabilities in aerial robotics.

6 REFERENCES

[1] Imanberdiyev, N., Sood, S., Kircali, D., & Kayacan, E. (2022). Design, development and experimental validation of

a lightweight dual-arm aerial manipulator with a COG balancing mechanism. *Mechatronics, 82*, 102719. https://doi.org/10.1016/j.mechatronics.2021.102719

[2] Simon, J., Petkovic, I., Petkovic, D., & Petkovics, Á. (2018). Navigation and applicability of hexa rotor drones in greenhouse environment. *Tehnicki vjesnik - Technical Gazette, 25*(2), 249-255. https://doi.org/10.17559/TV-20161109211133

[3] Suarez, A., Salmoral, R., Garofano-Soldado, A., Heredia, G., & Ollero, A. (2022). Aerial device delivery for power line inspection and maintenance. *Proc. IEEE International Conference on Unmanned Aircraft Systems(ICUAS)*, 30-38. https://doi.org/10.1109/ICUAS54217.2022.9836039

[4] Li, G., Ge, R., & Loianno, G. (2021). Cooperative transportation of cable suspended payloads with mavs using monocular vision and inertial sensing. *IEEE Robotics and Automation Letters, 6*(3), 5316-5323. https://doi.org/10.1109/LRA.2021.3065286

[5] Qian, L. & Liu, H. H. (2019). Path-following control of a quadrotor UAV with a cable-suspended payload under wind disturbances. *IEEE Transactions on Industrial Electronics, 67*(3), 2021-2029. https://doi.org/10.1109/TIE.2019.2905811

[6] Kišev, M., Vacho, L., Tóth, L., Olejár, M., Harničárová, M., Valíček, J., & Tozan, H. (2022). Experimental measurement of a UAV propeller's thrust. *Tehnicki vjesnik - Technical Gazette, 29*(1), 73-80. https://doi.org/10.17559/TV-20201212185220

[7] George, S. & Samuel, P. (2012). On the design and development of a coaxial nano rotorcraft. *50th AIAA Aerospace Sciences Meeting including the New Horizons Forum and Aerospace Exposition, 585*. https://doi.org/10.2514/6.2012-585

[8] Schafroth, D., Bouabdallah, S., Bermes, C., & Siegwart, R. (2009). From the test benches to the first prototype of the muFly micro helicopter. *Journal of Intelligent and Robotic Systems, 54*, 245-260. https://doi.org/10.1007/s10846-008-9264-z

[9] Zhang, J., Fei, F., Tu, Z., & Deng, X. (2017). Design optimization and system integration of robotic hummingbird. *Proc. of IEEE International Conference on Robotics and Automation (ICRA)*, 5422-5428. https://doi.org/10.1109/ICRA.2017.7989639

[10] Falanga, D., Kleber, K., Mintchev, S., Floreano, D., & Scaramuzza, D. (2018). The foldable drone: A morphing quadrotor that can squeeze and fly. *IEEE Robotics and Automation Letters, 4*(2), 209-216. https://doi.org/10.1109/LRA.2018.2885575

[11] Brunner, M., Bodie, K., Kamel, M., Pantic, M., Zhang, W., Nieto, J., & Siegwart, R. (2020). Trajectory tracking nonlinear model predictive control for an overactuated mav. *Proc. of IEEE International Conference on Robotics and Automation (ICRA)*, 5342-5348. https://doi.org/10.1109/ICRA40945.2020.9197005

[12] Prior, S. D. (2010). Reviewing and investigating the use of co-axial rotor systems in small UAVs. *International Journal of Micro Air Vehicles, 2*(1), 1-16. https://doi.org/10.1260/1756-8293.2.1.1

[13] Paulos, J. & Yim, M. (2013). An underactuated propeller for attitude control in micro air vehicles. *Proc. of IEEE/RSJ International Conference on Intelligent Robots and Systems*, 1374-1379. https://doi.org/10.1109/IROS.2013.6696528

[14] Paulos, J. & Yim, M. (2015). Flight performance of a swashplateless micro *a*ir vehicle. *Proc. of IEEE International Conference on Robotics and Automation (ICRA)*, 5284-5289. https://doi.org/10.1109/ICRA.2015.7139936

[15] Paulos, J., Caraher, B., & Yim, M. (2018). Emulatinga fully actuated aerial vehicle using two actuators. *Proc. of IEEE International Conference on Robotics and Automation(ICRA*), 7011-7016. https://doi.org/10.1109/ICRA.2018.8462975

[16] Paulos, J. & Yim, M. (2018). Cyclic blade pitch control without a swashplate for small helicopters. *Journal of Guidance, Control, and Dynamics, 41*(3), 689-700. https://doi.org/10.2514/1.G002683

[17] Qin, Y., Chen, N., Cai, Y., Xu, W., & Zhang, F. (2022). Gemini ii: Design, modeling, and control of a compact yet efficient servoless bi-copter. *IEEE/ASME Transactions on Mechatronics, 27*(6), 4304-4315. https://doi.org/10.1109/TMECH.2022.3153587

[18] Li, H., Chen, N., Kong, F., Zou, Y., Zhou, S., He, D., & Zhang, F. (2023). HALO: A Safe, Coaxial, and Dual-Ducted UAV Without Servo. *Proc. of IEEE/RSJ International Conference on Intelligent Robots and Systems (IROS)*, 6935-6941. https://doi.org/10.1109/IROS55552.2023.10341923

[19] Chen, N., Kong, F., Li, H., Liu, J., Ye, Z., Xu, W., Zhu, F., Lyu, X., & Zhang, F. (2023). Swashplateless-elevon Actuation for a Dual-rotor Tail-sitter VTOL UAV. *Proc. of IEEE/RSJ International Conference on Intelligent Robots and Systems (IROS)*, 6970-6976. https://doi.org/10.1109/IROS55552.2023.10341861

[20] Chen, N., Kong, F., Xu, W., Cai, Y., Li, H., He, D., Qin, Y., & Zhang, F. (2023). A self-rotating, single-actuated UAV with extended sensor field of view for autonomous navigation. *Science Robotics, 8*(76), eade4538. https://doi.org/10.1126/scirobotics.ade4538

Contact information:

Ali Tahir KARASAHIN
(Corresponding author)
Department of Mechatronics Engineering, Necmettin Erbakan University,
Konya42090, Turkey
E-mail: alitahir.karasahin@erbakan.edu.tr

Gokhan GUNGOR
Department of Mechatronics Engineering, Karabuk University,
Karabuk 78050, Turkey
E-mail: gokhangungor@karabuk.edu.tr